Available online at www.sciencedirect.com
ScienceDirect
Catalysis Today 121 (2007) 197–203
CATALYSIS TODAY
www.elsevier.com/locate/cattod

Micro-kinetic analysis of direct N_2O decomposition over steam-activated Fe-silicalite from transient experiments in the TAP reactor

Evgenii V. Kondratenko [a,*], Javier Pérez-Ramírez [b,*]

[a] *Leibniz-Institut für Katalyse e. V. an der Universität Rostock, Aussenstelle Berlin, Richard-Willstätter-Str. 12, D-12489 Berlin, Germany*
[b] *Laboratory for Heterogeneous Catalysis, Catalan Institution for Research and Advanced Studies (ICREA) and Institute of Chemical Research of Catalonia (ICIQ), Av. Països Catalans 16, E-43007, Tarragona, Spain*

Available online 17 October 2006

Abstract

Mechanistic and kinetic aspects of the direct decomposition of N_2O over steam-activated Fe-silicalite were investigated by transient experiments in vacuum (N_2O peak pressure of ca. 10 Pa) using the temporal analysis of products (TAP) reactor in the temperature range of 773–848 K. The transient responses of N_2O, N_2, and O_2 obtained upon N_2O decomposition were fitted to different micro-kinetic models. Through model discrimination it was concluded that both free iron sites and iron sites with adsorbed mono-atomic oxygen (*–O) species are active for N_2O decomposition. Oxygen formation occurs via decomposition of bi-atomic (*–O_2) oxygen species adsorbed over the iron site. This bi-atomic oxygen species originates from another bi-atomic oxygen species (O–*–O), which is initially formed via interaction of N_2O with iron site possessing mono-atomic oxygen species (*–O). Based on our modeling, the recombination of two mono-atomic oxygen (*–O) species or direct O_2 formation via reaction of N_2O with *–O can be excluded as potential reaction pathways yielding gas-phase O_2. The simulation results predict that the overall rate of N_2O decomposition is controlled by regeneration of free iron sites via a multi-step oxygen formation at least below 700 K.

Keywords: N_2O decomposition; Iron zeolites; Oxygen formation; Mechanism; Micro-kinetics; TAP reactor

1. Introduction

Since the pioneering work of Hall and co-workers [1], numerous studies of the mechanism and kinetics of direct N_2O decomposition over iron-containing zeolites have been published. They have been also stimulated by the potential applicability of Fe-ZSM-5 for N_2O abatement in tail gases of chemical production and combustion processes. It is well accepted that certain iron sites in the catalyst activate N_2O with formation of gas-phase N_2 and adsorbed oxygen species (Eq. (1)). Although there is wide agreement that O_2 formation is rate-determining step [1–6], there is no consensus on the reaction pathways leading to gas-phase O_2. Basically two descriptions have been put forward. Atomic oxygen species deposited over iron sites can recombine [3,4,7,8] to give gas-phase O_2 according to Eq. (2). Alternatively [1,9], N_2O can react with adsorbed oxygen species yielding gas-phase O_2 and N_2 (Eq. (3)).

$$N_2O + * \rightarrow N_2 + *{-}O \quad (1)$$

$$*{-}O + *{-}O \rightarrow 2* + O_2 \quad (2)$$

$$N_2O + *{-}O \rightarrow * + O_2 + N_2 \quad (3)$$

$$N_2O + *{-}O_2 \rightarrow * - O_3 + N_2 \quad (4)$$

$$*{-}O_3 \rightarrow * - O + O_2 \quad (5)$$

Recently, Heyden et al. [10] published a detailed mechanistic DFT investigation of N_2O decomposition over Fe-ZSM-5. An isolated iron site was assumed as an active center for N_2O decomposition. These authors identified that free iron sites as well as iron sites with one or two deposited oxygen species are active for N_2O decomposition. They concluded that the main reaction pathway for oxygen formation under steady-state conditions is the decomposition of tri-atomic oxygen species yielding an iron site with

* Corresponding authors.
E-mail addresses: evgenii@aca-berlin.de (E.V. Kondratenko), jperez@iciq.es (J. Pérez-Ramírez).

0920-5861/$ – see front matter © 2006 Elsevier B.V. All rights reserved.
doi:10.1016/j.cattod.2006.08.066

mono-atomic oxygen species (Eqs. (4) and (5)), which further participates in N_2O decomposition (Eq. (3)). Such a complex reaction mechanism is difficult to verify by means of steady-state experiments. Transient techniques have the potential of providing considerably more insights into elementary steps of catalyzed processes. Apart from the kinetic studies of high-temperature N_2O decomposition over noble metals [11,12], to the authors' knowledge there is no available literature on the application of the TAP (temporal analysis of products) reactor for micro-kinetic analysis of direct N_2O decomposition over iron-containing zeolites. However, the TAP reactor has been successfully applied to derive mechanistic insights into direct N_2O decomposition [3,13,14] and N_2O-mediated reactions [14,15] over Fe-MFI catalysts.

The present study is focused on the micro-kinetic analysis of N_2O decomposition over steam-activated Fe-silicalite under transient conditions in the TAP reactor. The analysis is based on simultaneous fitting of transient responses of N_2O, N_2, and O_2 to different kinetic models and discriminating between them. Particular emphasis is on deriving insights into the reaction pathways of O_2 formation and their role in the global reaction kinetics.

2. Experimental

2.1. Catalyst

Steam-activated Fe-silicalite (Si/Al $\sim \infty$ and 0.68 wt.% Fe) was prepared according to the procedure described elsewhere [16–18]. Characterization studies of this catalyst evidenced the predominance of isolated iron species and a relative low degree of iron clustering.

2.2. Transient experiments

Mechanistic investigations were carried out in the TAP-2 reactor, a transient pulse technique with sub-millisecond time resolution [19]. Fe-silicalite (50 mg, sieve fraction 250–350 μm) was packed in the quartz micro-reactor (40 mm length and 6 mm i.d.) between two layers of quartz particles of the same sieve fraction. Prior to the experiments, the catalyst was pretreated in flowing He (30 ml STP min^{-1}) at 773 K and atmospheric pressure for 2 h. The pre-treated sample was then exposed to vacuum (10^{-5} Pa) and the pulse experiments were subsequently performed. The direct N_2O decomposition was investigated in the temperature range of 773–848 K by pulsing an N_2O:Ne = 1:1 mixture. Knudsen diffusion describes the transport of the gas in the catalyst bed at the pulse size applied (5×10^{14} molecules). Under this regime, the transient responses are a function of gas-solid interactions, i.e. they are not influenced by eventual collisions of species in the gas phase.

Ne (99.995%) and N_2O (99.0%) were applied without additional purification. A quadrupole mass spectrometer (HAL RC 301 Hiden Analytical) was used for quantitative analysis of gaseous components. The transient responses at the reactor outlet were monitored at the following atomic mass units (AMU): 44 (N_2O), 32 (O_2), 30 (N_2O), 28 (N_2, N_2O), and 20 (Ne). In the experiments, 10 pulses were recorded and averaged for each AMU in order to improve the signal-to-noise ratio. The variations in feed components and reaction products were determined from the respective AMUs using standard fragmentation patterns and sensitivity factors.

2.3. Mathematical treatment of transient data

The micro-kinetic schemes of N_2O decomposition evaluated in this study are summarized in Table 1. Mass balances for gas-phase and surface species outside the catalyst layer can be expressed by Eqs. (6) and (7), respectively:

$$\frac{\partial C_i}{\partial t} = D^{\text{eff}}_{\text{Knudsen}} \times \frac{\partial^2 C_i}{\partial x^2} \tag{6}$$

$$\Theta_m = 0 \tag{7}$$

In the catalyst zone the reaction term is included in the mass balances for gas-phase (Eq. (8)) and surface (Eq. (9)) species:

$$\frac{\partial C_i}{\partial t} = D^{\text{eff}}_{\text{Knudsen}} \times \frac{\partial^2 C_i}{\partial x^2} + \sum_j \rho_{\text{cat}} \nu_{ij} r_j \tag{8}$$

$$\frac{\partial \Theta_m}{\partial t} = \sum_j \frac{\nu_{ij} r_j}{C_{\text{total}}} \tag{9}$$

Table 1
Reaction schemes for direct N_2O decomposition evaluated in this study

Number	Elementary reaction steps	
1	$N_2O + * \rightarrow N_2 + *-O$	(1)
	$*-O + *-O \rightarrow O_2 + 2*$	(2)
2	$N_2O + * \rightarrow N_2 + *-O$	(1)
	$N_2O + *-O \rightarrow N_2 + O_2 + *$	(2)
3	$N_2O + * \rightarrow N_2 + *-O$	(1)
	$*-O + *-O \rightarrow *-O_2 + *$	(2)
	$*-O_2 \rightarrow O_2 + *$	(3)
4	$N_2O + * \rightarrow N_2 + *-O$	(1)
	$N_2O + *-O \rightarrow N_2 + *-O_2$	(2)
	$*-O_2 \rightarrow O_2 + *$	(3)
5	$N_2O + * \rightarrow *-O + N_2$	(1)
	$N_2O + *-O \rightarrow O-*-O + N_2$	(2)
	$O-*-O \rightarrow *-O_2$	(3)
	$*-O_2 \rightarrow O_2 + *$	(4)
6	$N_2O + * \rightarrow *-O + N_2$	(1)
	$N_2O + *-O \rightarrow *-O_2 + N_2$	(2)
	$N_2O + *-O_2 \rightarrow *-O_3 + N_2$	(3)
	$*-O_2 \rightarrow O_2 + *$	(4)
	$*-O_3 \rightarrow O_2 + *-O$	(5)

where $r_j = k_j \prod_i C_i^{n_1} \prod_m \theta_m^{n_m}$, $0 \le n_i \le 1$, $0 \le n_m \le 2$, $1 = \sum \Theta_m$, $\Theta_m = C_m / C_{\text{total}}$, C_{total} is the total concentration of surface sites and D_{eff} is the effective Knudsen diffusion coefficient of gas-phase species. The intracrystalline diffusion was not taken into consideration in the model. This simplification is based on the previous work of Keipert and Baerns [20], who showed that this process has a very slight influence on the shape of transient responses of inert gases upon pulsing in the TAP reactor. The transport behaviour of oxygen and nitrogen (products of N_2O decomposition) may be considered to be similar to inert gases. Therefore, the transport of gases inside the micro reactor was described by Knudsen diffusion in the axial direction.

The parameter estimation procedure used here was described elsewhere [21,22]. Briefly, it is based on a numerical solution of partial differential equations (PDEs) describing processes of diffusional transport, adsorption/desorption, and reaction in the micro-reactor. PDEs are transformed into coupled ordinary differential equations (ODEs) by a spatial approximation and then integrated numerically using the PDEONE routine [23]. Parameters were determined using first a genetic algorithm to find good starting values [24] and then the Nelder–Mead simplex algorithm [25]. The micro-reactor was described as a one-dimensional pseudo-homogeneous system divided into three different zones, which are represented by the catalyst and the two layers of inert material where the zeolite was sandwiched. The catalyst is located in the isothermal zone of the reactor. The goodness of fit was characterized by an objective function defined as the sum of squares of the shortest deviation between the respective pairs of points of the experimental and simulated transient responses [22]. For simultaneous fitting of transient responses of various intensities, the number of the representative points for low-intensity responses was higher than for high-intensity ones. This procedure is useful in order to minimize the influence of highly intensive responses on the objective function.

In order to calculate confidence limits of the determined parameters, a sensitivity analysis was applied. Accordingly, the software changed the parameter until 10% change of the objective function was achieved.

3. Results and discussion

3.1. N_2O decomposition under transient conditions

Steam-activated Fe-silicalite is active for direct N_2O decomposition under steady-state ambient pressure [17] and transient vacuum conditions [14]. Gas-phase N_2 was observed starting from 523 K. However, no gas-phase oxygen was detected below 623 K. Typical transient responses of N_2O, N_2, and O_2 obtained upon N_2O pulsing over Fe-silicalite at 773 K are illustrated in Fig. 1. Each transient response has a unique mean residence time, temporal maximum, and decay. The transient response of N_2O appears at the shortest time interval and has the fastest decay. The transient response of N_2 is somewhat broader and is slightly shifted to longer times with respect to N_2O. The O_2 response is substantially broader

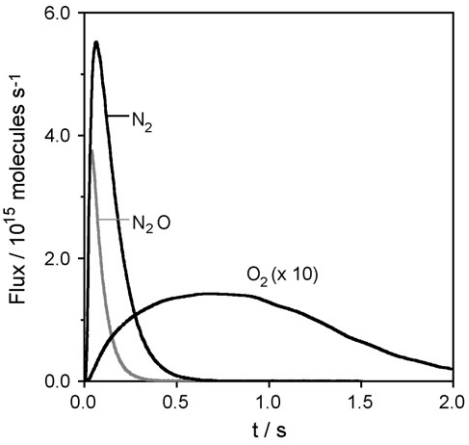

Fig. 1. Transient responses of N_2O, N_2, and O_2 upon N_2O decomposition over Fe-silicalite at 773 K.

than that of N_2 and its maximum is shifted to much longer times. The O_2 response does not come to zero intensity even after ca. 2 s. Since the time of the maximum ($t_{\max}$) of the transient responses is related to the reaction kinetics [19], valuable insights into relative rates of N_2 and O_2 formation from N_2O can be obtained from the analysis of the respective maxima. Fig. 2 shows the $t_{\max}$ values for O_2 and N_2 responses at different temperatures. It is evidenced that $t_{\max}$ of N_2 is one order of magnitude smaller than $t_{\max}$ of O_2. Moreover, $t_{\max}$ of O_2 decreases from 0.56 to 0.17 s upon increasing reaction temperature from 773 to 848 K, while the corresponding change in $t_{\max}$ of N_2 is much less pronounced (from 0.065 to 0.046 s). In agreement with our previous observations [3,13,14], it can be concluded that: (i) N_2 formation is much faster than O_2 formation, and (ii) the activation energy of reaction pathways leading to O_2 is higher than those leading to N_2.

3.2. Micro-kinetics of N_2O decomposition

In order to derive kinetic insights into direct N_2O decomposition over Fe-silicalite under transient conditions,

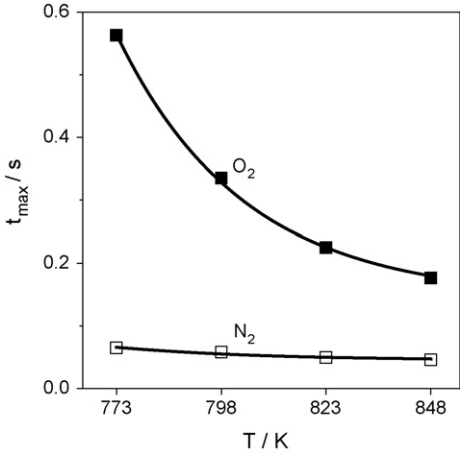

Fig. 2. Time of maximum ($t_{\max}$) of the transient responses of O_2 and N_2 vs temperature upon N_2O decomposition over Fe-silicalite.

the experimental transient responses of reactant (N_2O) and reaction products (O_2 and N_2) were simultaneously fitted to different micro-kinetic models, which are summarized in Table 1. The elementary reaction steps implemented in these models were selected from literature data for iron-containing zeolites [1,6,8,10,26–29]. The models were tested in the order of increasing complexity. Model discrimination was performed at a reference temperature of 798 K. According to [30] the reference temperature should be centered within the temperature range applied, which was between 773 and 848 K in our study.

For all models, N_2O decomposition is initiated by the reaction of gas-phase N_2O with free iron site yielding reactive atomic oxygen species (*–O). No information on the charge of this oxygen species can be derived from the applied fitting procedure. Model 2 considers O_2 formation via reaction of gas-phase N_2O with the oxygen species (*–O) according to [1,9]. Contrarily, model 1 considers that gas-phase oxygen is formed via recombination of two oxygen (*–O) species [3,4,7,8]. The results of the kinetic evaluation in Fig. 3 evidence that models 1 and 2 do not reproduce correctly the measured transient responses of N_2O, N_2, and O_2. The above models were slightly modified considering that oxygen formation occurs via decomposition of a molecular oxygen precursor (*–O_2) as previously suggested for Fe-MFI [6] and for Cu-ZSM-5 [9]. This molecularly adsorbed oxygen species was assumed to be formed either by recombination of two atomic oxygen species (model 3) or by reaction of gas-phase N_2O with oxygen species (*–O) (model 4). Without conclusive statements on the nature of oxygen species, the existence of two different types of oxygen species was suggested in our previous analysis of O_2-C_3H_8 [13] and O_2-CH_4 [15] interactions over Fe-silicalite in the TAP reactor applying sequential pulse experiments with different time delays between N_2O and the reducing agent. This concept is also in line with the results of Kunimori and co-workers [31–33], who postulated two types of oxygen species originated upon N_2O activation over Fe-beta during selective catalytic reduction (SCR) of N_2O with CH_4. The comparison of experimental and predicted transient responses assuming models 3 and 4 is given in Fig. 3. These models did not provide a proper representation of the experimental data.

Consequently, the mechanism of oxygen formation was modified in models 5 and 6. These models are based on the recent DFT study of direct N_2O decomposition over isolated iron species in Fe-ZSM-5 [10]. These authors postulated three types of adsorbed oxygen species: mono-atomic, bi-atomic, and tri-atomic. N_2O can decompose on free iron sites as well as on iron sites with mono-atomic and bi-atomic oxygen species, i.e. Fe^{2+}, Fe^{2+}–O, Fe^{2+}–O_2 species. In our study, model 5 considers two types of bi-atomic oxygen species, one of which is formed via reaction of N_2O with mono-atomic oxygen species (*–O) originated upon N_2O decomposition over free iron sites (Table 1, step 2 in model 5) followed by its transformation into a bi-atomic oxygen species with a different structure (Table 1, step 3 in model 5). Free iron sites (*), iron sites with mono-atomic (*–O) and bi-atomic (*–O_2) oxygen species can react with gas-phase N_2O yielding mono-atomic oxygen species (Table 1, step 1 in mode 6), bi-atomic oxygen species (Table 1, step 2 in model 6), and tri-atomic oxygen species (Table 1, step 3 in model 6), respectively. Decomposition of bi- and tri-atomic

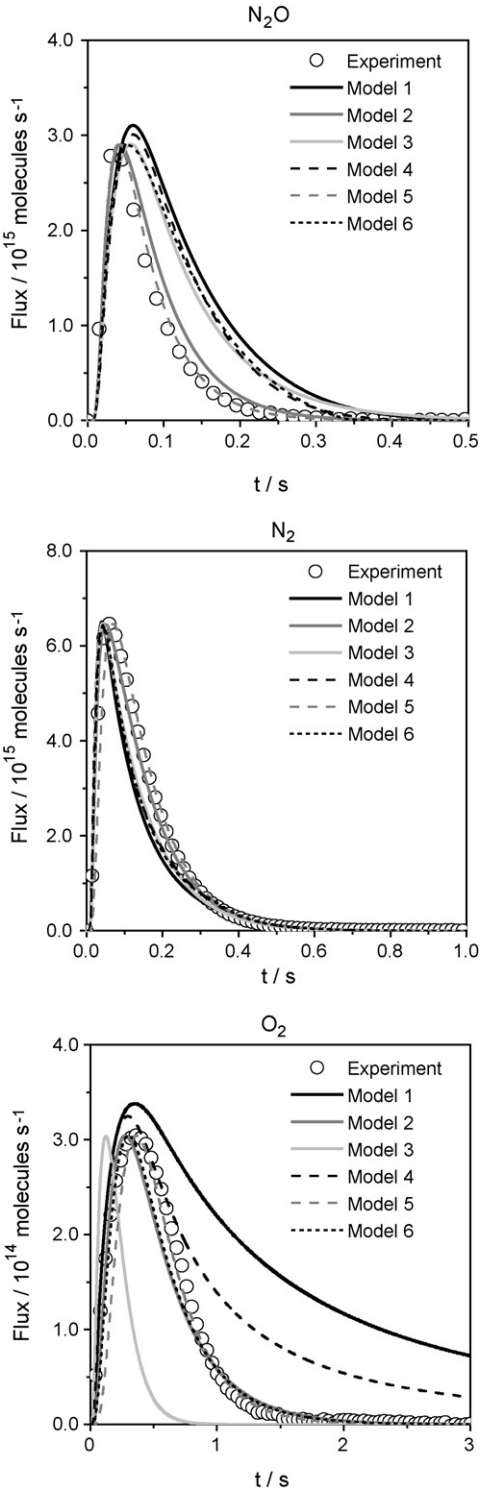

Fig. 3. Comparison between the experimental (symbols) and predicted (lines) transient responses of N_2O, N_2, and O_2 upon N_2O decomposition over Fe-silicalite at 798 K.

oxygen species yields gas-phase O_2 (Table 1, steps 4 and 5 in model 6).

The smallest deviations between the experimental and predicted transient responses of N_2O, N_2, and O_2 were obtained with model 5 (Fig. 3). As mentioned above, this model considers the existence of two different bi-atomic oxygen species. Based on the recent DFT calculations by Heyden et al. [10], bi-atomic oxygen species formed upon N_2O decomposition over mono-atomic oxygen species (Table 1, step 2 in model 5) may have an O–Fe–O structure, i.e. without any chemical bond between the oxygen atoms. This bi-atomic species is transformed to another bi-atomic oxygen species (Table 1, step 3 in model 5), where the oxygen atoms are chemically bonded and one or both oxygen atoms are bound to the iron center. To determine the exact structure of this species goes beyond the modeling approach used in our paper.

The correct prediction of measured data over a broad temperature range is an important validation criteria. Therefore, the temperature dependency of elementary reaction pathways in model 5 was elucidated by simultaneously fitting transient responses of N_2O, N_2, and O_2 obtained upon N_2O decomposition at four temperatures in the range of 773–848 K. To reduce the correlation between activation energies and pre-exponential factors [30,34], activation energies for all elementary reaction steps were derived according to Eq. (10).

$$k_{T_i} = k_{T_{\mathrm{ref}}} \times \exp\left(-\frac{E_a}{R}\left(\frac{1}{T_i} - \frac{1}{T_{\mathrm{ref}}}\right)\right) \quad (10)$$

where T_{ref} and $k_{T_{\mathrm{ref}}}$ are the reference temperature and the rate coefficient at this temperature, respectively. The constants at the reference temperature were initially obtained from fitting as described above and fixed in the subsequent calculations.

The parity plot with the experimental and predicted fluxes is shown in Fig. 4. The agreement between measured and calculated values is excellent. The optimized values for kinetic parameters in model 5 are listed in Table 2. It has to be stressed

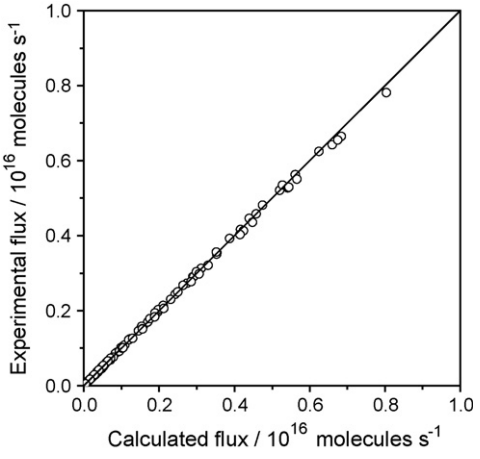

Fig. 4. Parity plot of the experimental and predicted fluxes of N_2O, N_2, and O_2 upon N_2O decomposition over Fe-silicalite in the temperature range of 773–848 K.

Table 2
Optimized kinetic parameters and their confidence limits[a] for the elementary reaction steps of N_2O decomposition over Fe-silicalite according to model 5

No	Elementary step	$k_{798\ \mathrm{K}}$ (s^{-1})	E_a (kJ mol^{-1})
1	$N_2O + * \rightarrow *\text{–}O + N_2$	1170[b] ± 68	120 ± 8
2	$N_2O + *\text{–}O \rightarrow O\text{–}*\text{–}O + N_2$	167[b] ± 9.5	81 ± 8
3	$O\text{–}*\text{–}O \rightarrow *\text{–}O_2$	26 ± 5.5	298 ± 44
4	$*\text{–}O_2 \rightarrow O_2 + *$	2.7 ± 0.1	129 ± 8

[a] Confidence limits were calculated by varying the optimized parameters in the fitting procedure until 10% change of the objective function was achieved.
[b] For these reaction steps, the rate coefficient is the product of the intrinsic rate coefficient and the total number of active sites.

that apparent kinetic constants ($k_i \times C_{\mathrm{total}}$) were determined for reaction pathways 1 and 2, since it is not possible to determine independently the intrinsic rate constants and the total number of surface sites. It is clear that the reaction pathway of oxygen desorption has the lowest rate coefficient, i.e. oxygen desorption can be considered as the rate-limiting step in direct N_2O decomposition in agreement with literature [1–6]. Moreover, the activation energies of reaction pathways resulting in O_2 formation are considerably higher than those for N_2 formation. This is in excellent agreement with the experimental observations in Fig. 2, which shows that $t_{\max}$ of the O_2 response is more affected by temperature than the N_2 response.

3.3. Simulation of steady-state experiments

In order to analyze whether O_2 formation determines the overall rate of N_2O decomposition under steady-state conditions, surface coverages at different temperatures and N_2O partial pressures were simulated using the kinetic parameters in Table 2. To this end, it was assumed that all iron species in the catalyst were available and active for direct N_2O decomposition. Using the software Maple V [35], the steady-state coverage by free Fe-sites as well as mono- (*–O) and bi-atomic (O–*–O and *–O_2) oxygen species were computed from the set of algebraic equations (steps 1–4 in model 5, Table 1) and site balance equation ($1 = \Theta_{*-O} + \Theta_{*-O_2} + \Theta_{O-*-O} + \Theta_{*}$). Fig. 5 illustrates the coverages by different species at different N_2O partial pressures (0.01–10 kPa) and temperatures of 598 and 798 K. It is clearly observed that Fe-sites are practically covered by bi-atomic oxygen species (O–*–O) at 598 K in a very broad range of N_2O partial pressures. According to our model, the iron site with bi-atomic oxygen species do not participate in N_2O decomposition, so it is not expected for Fe-silicalite to be active in the reaction at this temperature. As previously reported by [14], no gas-phase oxygen was observed upon N_2O multi-pulse experiments in the TAP reactor over steam-activated Fe-silicalite below 673 K. High N_2O conversion was observed in the first pulse and continuously decreased approaching zero after ca. 300 N_2O pulses. This experimental behavior can be explained by blocking of active sites for N_2O decomposition (free iron sites and iron sites with mono-atomic oxygen species) with bi-atomic ones, which do not decompose at low temperatures. Upon increasing the reaction temperature,

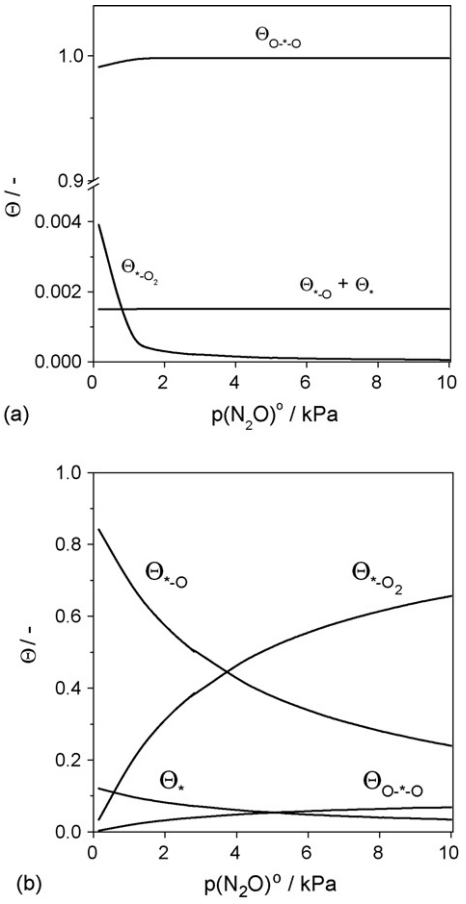

Fig. 5. Dependence of the calculated surface coverages (model 5) over Fe-silicalite on the inlet partial pressure of N_2O at (a) 598 K and (b) 798 K.

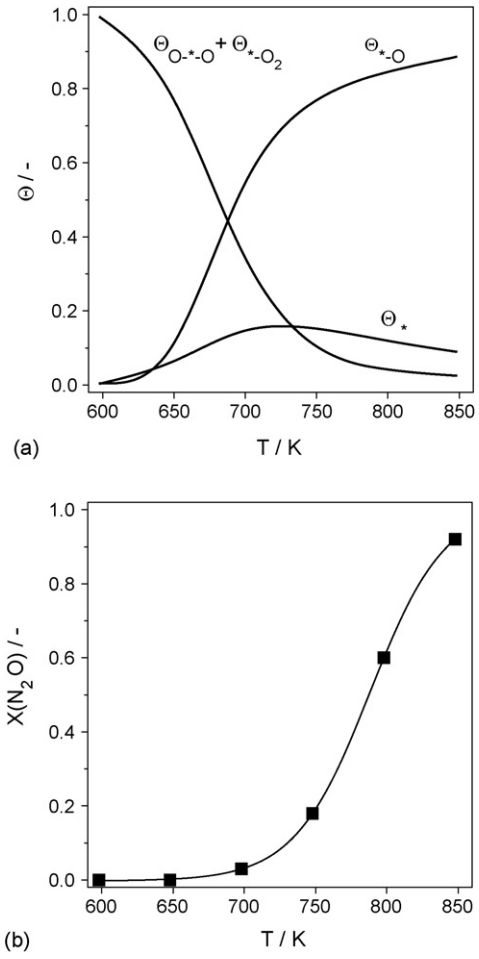

Fig. 6. Calculated coverage of surface species according to model 5 (a) and N_2O conversion (b) versus temperature at $p(N_2O)^\circ = 0.15$ kPa. Values of N_2O conversion weretaken from [17].

the coverage by iron sites with bi-atomic oxygen species decreases (Fig. 5). The decrease in this coverage is related to the temperature-accelerated O_2 desorption. Oxygen starts to be formed above 673 K under the present transient conditions. The importance of oxygen desorption in N_2O decomposition under steady-state conditions can be illustrated by the following example. Fig. 6 compares changes in the calculated coverage by free iron sites, iron sites with mono- and bi-atomic oxygen species as well as the experimental N_2O conversion with temperature [17]. The coverage was computed for N_2O partial pressure of 0.15 kPa, at which the steady-state performance was measured. The figure shows that the coverage by iron sites with bi-atomic oxygen species decreases from 1 to ca. 0.02 with an increase in temperature from 598 to 848 K. For the respective temperature changes, the N_2O conversion and the coverage by mono-atomic oxygen species increased from 0 to ca. 0.9, and from ca. 0.04 to ca. 0.9, respectively. The coverage by free iron sites passes over a maximum between 700 and 750 K.

Summarizing the above results it can be concluded that the derived micro-kinetic model of direct N_2O decomposition describes transient performance of Fe-silicalite in the temperature range of 773–848 K. Steady-state performance of Fe-silicalite can be also qualitatively predicted by the model.

4. Conclusions

Several micro-kinetic models were evaluated and discriminated in order to describe the transient responses of N_2O, N_2, and O_2 during direct N_2O decomposition over steam-activated Fe-silicalite in the Temporal Analysis of Products (TAP) reactor. The best model consists of four elementary steps, indicating the complexity of O_2 formation in the overall mechanism. N_2O decomposes both over free iron sites (*) and iron sites with deposited mono-atomic oxygen species (*–O). The latter reaction pathway originates a bi-atomic oxygen precursor (O–*–O). This precursor transforms into another bi-atomic oxygen species (*–O_2), which decomposes yielding gas-phase oxygen and a free iron site. Reaction pathways used classically to explain O_2 formation via reaction of N_2O with adsorbed mono-atomic oxygen species (*–O) or via recombination of *–O can be excluded. Moreover, it can be concluded that regeneration of free iron sites via multi-step transformations of bi-atomic adsorbed oxygen species to gas-phase O_2 really limits the overall rate of N_2O decomposition over Fe-silicalite at least below 700 K under both transient and steady-state conditions.

Acknowledgements

EVK thanks financial support from the Deutsche Forschungsgemeinschaft (DFG) in the frame of the competence network (Sonderforschungsbereich 546) ''Structure, dynamics and reactivity of transition metal oxide aggregates''. JPR thanks financial support from the Spanish DGICYT (Project CTQ2006-01562/PPQ).

References

[1] C.M. Fu, V.N. Korchak, W.K. Hall, J. Catal. 68 (1981) 166.
[2] G. Mul, J. Pérez-Ramírez, F. Kapteijn, J.A. Moulijn, Catal. Lett. 77 (2001) 7.
[3] J. Pérez-Ramírez, G. Mul, F. Kapteijn, J.A. Moulijn, J. Catal. 208 (2002) 211.
[4] L. Kiwi-Minsker, D.A. Bulushev, A. Renken, J. Catal. 219 (2003) 273.
[5] G.D. Pirngruber, J. Catal. 219 (2003) 456.
[6] B.R. Wood, J.A. Reimer, A.T. Bell, M.T. Janicke, K.C. Ott, J. Catal. 224 (2004) 148.
[7] G.D. Pirngruber, M. Luechinger, P.K. Roy, A. Cecchetto, P. Smirniotis, J. Catal. 224 (2004) 429.
[8] L. Kiwi-Minsker, D.A. Bulushev, A. Renken, Catal. Today 110 (2005) 191.
[9] F. Kapteijn, G. Marban, J. Rodriguez-Mirasol, J.A. Moulijn, J. Catal. 167 (1997) 256.
[10] A. Heyden, F.J. Keil, B. Peters, A.T. Bell, J. Phys. Chem. B 109 (2005) 1857.
[11] E.V. Kondratenko, J. Pérez-Ramírez, Catal. Lett. 91 (2003) 211.
[12] V.A. Kondratenko, M. Baerns, J. Catal. 225 (2004) 37.
[13] E.V. Kondratenko, J. Pérez-Ramírez, Appl. Catal. A 267 (2004) 181.
[14] J. Pérez-Ramírez, E.V. Kondratenko, M.N. Debbagh, J. Catal. 233 (2005) 442.
[15] E.V. Kondratenko, J. Pérez-Ramírez, Appl. Catal. B 64 (2006) 35.
[16] J. Pérez-Ramírez, G. Mul, F. Kapteijn, J.A. Moulijn, A.R. Overweg, A. Doménech, A. Ribera, I.W.C.E. Arends, J. Catal. 207 (2002) 113.
[17] J. Pérez-Ramírez, F. Kapteijn, J.C. Groen, A. Doménech, G. Mul, J.A. Moulijn, J. Catal. 214 (2003) 33.
[18] J. Pérez-Ramírez, F. Kapteijn, A. Brückner, J. Catal. 218 (2003) 234.
[19] J.T. Gleaves, G.S. Yablonsky, P. Phanawadee, Y. Schuurman, Appl. Catal. A 160 (1997) 55.
[20] O.P. Keipert, M. Baerns, Chem. Eng. Sci. 53 (1998) 3623.
[21] M. Rothaemel, PhD Thesis, Ruhr-Universität Bochum, Bochum, 1995, p. 140.
[22] M. Soick, D. Wolf, M. Baerns, Chem. Eng. Sci. 55 (2000) 2875.
[23] R.F. Sinkovek, N.K. Madsen, ACM Trans. Math. Software 1 (1975) 232.
[24] D. Wolf, R. Moros, Chem. Eng. Sci. 52 (1997) 1189.
[25] W.H. Press, B.P. Flannery, S.A. Teukolsky, W.T. Vetterling, Numerical Recipes in FORTRAN, Cambridge University Press, Cambridge, 1992, 402.
[26] F. Kapteijn, J. Rodriguez-Mirasol, J.A. Moulijn, Appl. Catal. B 9 (1996) 25.
[27] D.A. Bulushev, L. Kiwi-Minsker, A. Renken, J. Catal. 222 (2004) 389.
[28] G.D. Pirngruber, P.K. Roy, Catal. Today 110 (2005) 199.
[29] A. Heyden, A.T. Bell, F.J. Keil, J. Catal. 233 (2005) 26.
[30] G.E.P. Box, N.R. Draper, Empirical Model-Building and Response Surfaces, Wiley & Sons, New York, 1987.
[31] S. Kameoka, T. Nobukawa, S. Tanaka, S. Ito, K. Tomishige, K. Kunimori, Phys. Chem. Chem. Phys. 5 (2003) 3328.
[32] T. Nobukawa, M. Yoshida, S. Kameoka, S.-i. Ito, K.i. Tomishige, K. Kunimori, Catal. Today 93–95 (2004) 791.
[33] T. Nobukawa, M. Yoshida, S. Kameoka, S.-i. Ito, K. Tomishige, K. Kunimori, J. Phys. Chem. B 108 (2004) 4071.
[34] D.M. Bates, D.G. Watts, Nonlinear Regression Analysis and its Application, John Wiley & Sons, New York, 1988.
[35] Waterloo Maple Inc., Maple 5, Release 5, 1998.